THE EFFECTS OF LIDAR DSM GRID RESOLUTION ON CATEGORISING RESIDENTIAL AND INDUSTRIAL BUILDINGS

J. Jaafar, G. Priestnall and P.M. Mather
School of Geography
The University of Nottingham
England
jaafar@geography.nottingham.ac.uk
gary.priestnall@nottingham.ac.uk
paul.mather@nottingham.ac.uk

KEY WORDS: LIDAR, DSM, 3D Surface Models, RMSE, Resolution, Classification, Land Use.

ABSTRACT

This paper reports the initial results of an analysis of LIDAR data using statistical methods in an attempt to categorise residential and industrial buildings. Two study sites representing these two land uses are identified. 3D models for the study area are constructed using an integrated methodology utilising the building polygons from digital map data and a LIDAR Digital Surface Model (DSM). The effects of LIDAR DSM grid resolution on the construction of the 3D model are analysed. Using statistics such as the Root Mean Square Error (*RMSE*) of the derived models at various LIDAR grid resolutions, the nature of building roofs in the residential and the industrial areas are identified. The height differences between the derived height and control height adopted for the 3D models are also determined for categorising the two building types. The Standard Deviation (*Std. Dev*.) of building height at various LIDAR DSM grid resolutions is also investigated as a discriminating measure. It is found that, due to the nature of the roof types that correspond to residential and industrial buildings, a classification of building types is possible.

1 INTRODUCTION

LIDAR (LIght Detection And Ranging) has become an established technique for deriving geometric information in three dimensions with decimetre accuracy (Lohr, 1998, Wehr and Lohr, 1999). Using this new technique, accurate Digital Surface Models (DSM) which portray both the grounds surface and the above surface features can be constructed in a relatively short time. A diversity of applications, which utilise LIDAR datasets is described by Gruen *et al.* (1995, 1997). Among these applications is the automatic generation of 3D models of buildings and other man-made objects, and the construction of Digital Elevation Models (DEMs) by 'stripping off' the above surface features (Hug, 1996, Jaafar *et al*., 1999a).

The fusion of available 2D vector databases with LIDAR DSMs offers the potential for rapid construction of 3D models (Haala, 1999, Jaafar *et al.*, 1999b) which potentially can be of benefit in various applications. However, this approach results in 3D models with flat roofs (Jaafar *et al.*, 1999b), unless the building primitives which constitute the geometry of the roof shape are well defined or determined from the LIDAR DSM (Haala, 1999). Understanding the nature of the roof top (which can be flat, gable or complex) could play an important role in categorising building types, and therefore in distinguishing residential from industrial land use. Jaafar *et al.* (1999b) suggest that, by experimenting with the LIDAR DSM resolution for the construction of the 3D model, the nature of the roof types of individual buildings could be revealed to some extent.

In this study, 3D models are generated using an integrated methodology (Jaafar *et al.*, 1999b) based on 2D building polygons and a LIDAR DSM. Samples of buildings that correspond to residential and industrial areas, which have different types of roof structure, are identified. The effects of the grid resolution of the LIDAR DSM in the creation of 3D models using the integrated methodology are analysed. The Root Mean Square Error (*RMSE*) between the derived height (maximum or mean) retrieved from the LIDAR DSM at various grid resolutions and the reference height (mean or maximum) at 2m resolution is computed for each of the samples identified. The result portrays the *RMSE* with respect to building type that will help categorise residential and industrial built up areas. Apart from assessing the effects on *RMSE*, the standard deviation of the building heights derived from the LIDAR DSM at various grid resolutions is also analysed. The result of this analysis may suggest the optimum grid resolution of LIDAR datasets for use in differentiating residential and industrial land uses.

2 THE NATURE OF THE DATA

LIDAR coverage was supplied by the UK Environment Agency for an area of the Trent floodplain covering the West Bridgford residential area and the Colwick Industrial Estate, Nottinghamshire, England. The areal coverage for each scene is 2km x 2km with a spatial resolution of 2m. The accuracy of the LIDAR dataset in this study is reported to be ± 0.20m (Jaafar *et al*., 1999a).

The residential buildings have complex roof structures of varying heights and sizes. Figure 1 shows the distribution of residential buildings shown on the LIDAR DSM, and Figure 2 shows the surface profile for a residential building. On the other hand, industrial buildings generally cover a larger surface area and have a simpler roof structure than residential buildings. Figure 3 shows the distribution of industrial buildings on the LIDAR DSM and Figure 4 portrays the surface profile for an industrial building.

Since the integrated methodology adopted from Jaafar *et al.* (1999b) requires 2D building polygons, the polygonal data structure was prepared from 1:1250 Ordnance Survey of Great Britain (OSGB). Using the Build command available in the ARC/INFO GIS, the Landline data were transformed to building polygons. Figure 5 and Figure 6 show the building polygons created for the residential and the industrial area respectively.

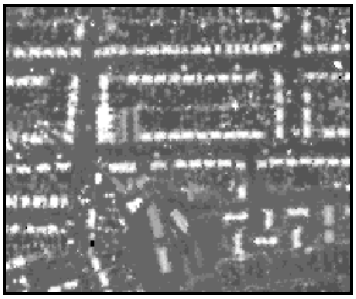

Figure 1: Distribution of residential buildings (*white*) on the LIDAR DSM (residential site).

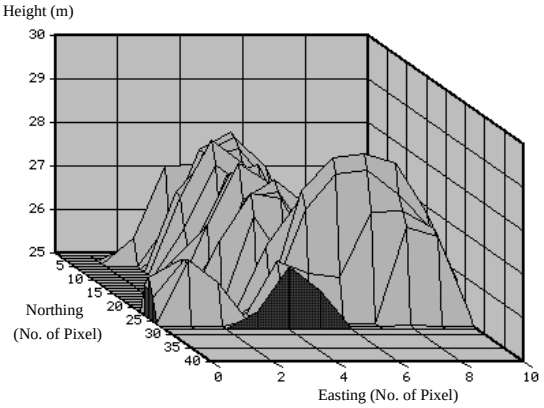

Figure 2: Example of the surface profile for a residential building derived from LIDAR data.

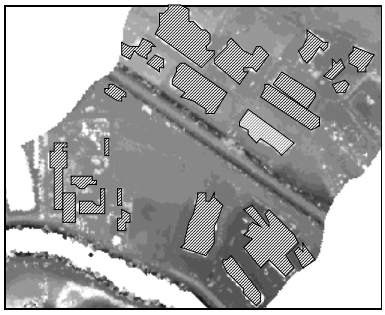

Figure 3: Distribution of industrial building (*shaded*) on the LIDAR DSM (industrial site).

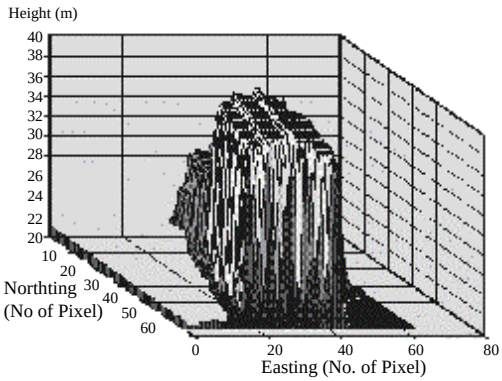

Figure 4: An example for the surface profile for an industrial building derived from LIDAR data.

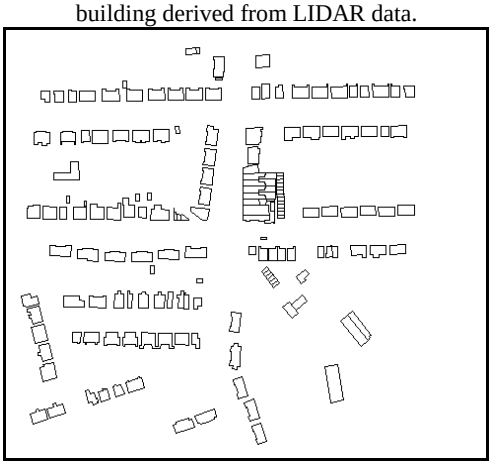

Figure 5: Building polygons for residential area derived from OSGB Landline data (Reproduced from Ordnance Survey mapping with the permission of The Controller of Her Majesty's Stationery Office, Crown Copyright. ED 273554).

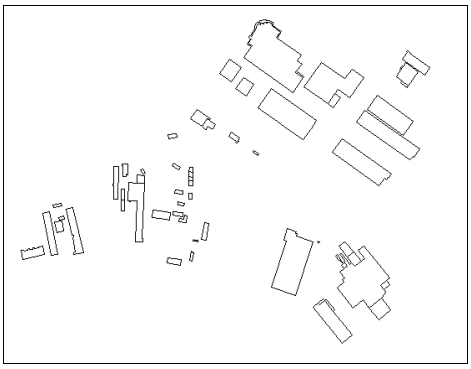

Figure 6: Building polygons for industrial area derived from OSGB Landline data (Reproduced from Ordnance Survey mapping with the permission of The Controller of Her Majesty's Stationery Office, Crown Copyright. ED 273554).

3 METHODOLOGY

Figures 2 and 4 shows that there is an observable difference between the surface profiles of residential and industrial buildings. The hypothesis posed here is that these differences can be characterised through the use of simple statistics that will

allow the identification of the two main types of building (residential and industrial) .

In this study, the magnitude of the *RMSE* for the derived 3D models at various grid resolutions is analysed. In addition to the *RMSE*, the value of standard deviation (*Std. Dev*.) of the building heights at various LIDAR DSM grid resolutions is also investigated. In the first part of the study, the initial 2m-grid LIDAR DSM is degraded to lower resolutions between 4m and 20m with a 2m-grid interval. Samples that represent residential and industrial building are then randomly identified for the computation of *RMSE* and *Std. Dev*. The number of buildings selected to represent residential and industrial buildings is 35 and 7 respectively.

In the next stage, 3D models for the study area using the heights derived from the LIDAR DSM for resolutions between 2m and 20m, with a 2m-grid interval, are constructed. As an example, Figure 7 and Figure 8 illustrate the basic concept for the integrated methodology using the building polygon and the LIDAR DSM data for the construction of the 3D model. Figure 7 shows how the maximum height encountered within the building polygon is extracted from the LIDAR DSM and is used to construct the 3D model. Figure 8 shows the resulting 3D model. Further discussion of this integrated methodology can be found in Jaafar *et al.* (1999b).

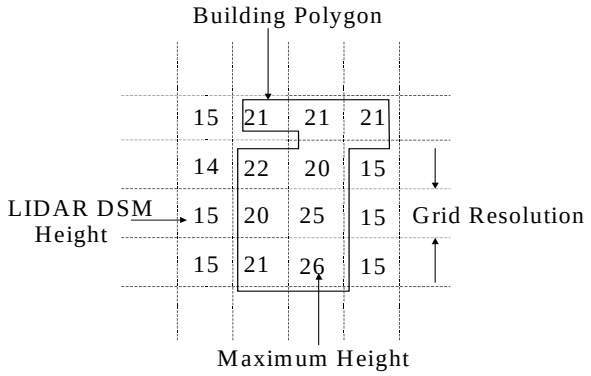

Figure 7: Maximum height retrieved from the LIDAR DSM for the construction of the 3D model.

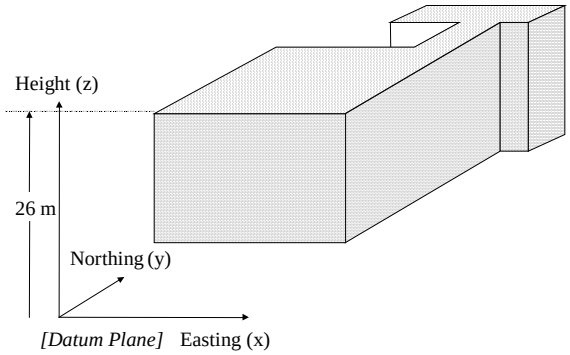

Figure 8: 3D model derived from the integrated methodology (Maximum height derived from LIDAR DSM).

3.1 Root Mean Square Error (*RMSE*)

Equation 1 shows the formula used for the computation of the *RMSE*.

$$RMSE = \sqrt{\left[\frac{1}{n}\sum_{i=1}^{n}\left(Z_i^* - Z_i\right)^2\right]} \qquad [1]$$

where n is the number of check points; Z^*_i is the 3D model height at position i and Z_i is the value of the 'control height' at check point i.

Since the computation of *RMSE* is based on the discrepancies between the height derived from the constructed 3D model and the reference height (control height) at specified positions, the control heights need to be determined.

In this study, control heights based on ground survey are not available. However, since it is the differences in the complexity of the roof structures of residential and industrial buildings that are being investigated, and not their absolute heights, the control heights were collected as follows;

Case I

In Case I, the effects on the 3D model constructed using the maximum height derived from the LIDAR DSM at various grid resolutions are analysed, using control heights taken as the height of a 3D model constructed using the mean height derived from the 2m-grid resolution LIDAR DSM. The 2m-grid resolution LIDAR DSM acts as a 'datum' as the greatest number of LIDAR surveyed points (X,Y,Z) are used to represent the DSM. It is considered to be the most accurate DSM available in this study. Since the mean height is adopted as the control height, the *RMSE* is based on the difference in vertical roof height between the maximum and the mean height for the constructed 3D model. Figure 9 shows the relationship between the building heights for the computation of *RMSE*. The hypothesis posed is that, if the difference in vertical roof height for both building types is not significant, the computed roof height will be constant even though the 3D models are constructed with varying grid resolutions. Section 4.1 discusses the results based on this hypothesis.

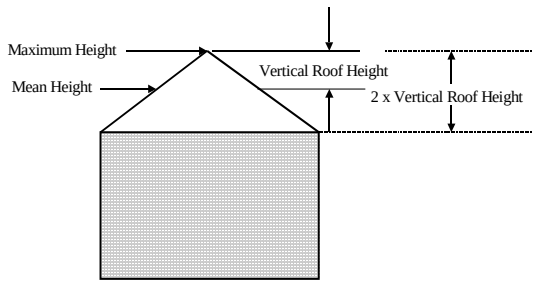

Figure 9: Relationship between the building heights for computation of *RMSE*.

Case II

Here, the averaging effect on the LIDAR DSM within the building polygons used to construct the 3D model is analysed. In this case, 3D models are constructed using the mean height derived from the LIDAR DSM at various grid resolutions. The control height adopted is similar to Case I. The hypothesis posed is that, if the building roof is not complex (flat roof), the *RMSE* should be constant even though the 3D model was constructed with varying grid resolutions. The advantages in this case will be, apart from understanding the nature of the vertical roof height through analysing the effect of *RMSE*, the *RMSE* will also give an accuracy estimate of the derived model with respect to the control height. The role of grid resolution in preserving the accuracy estimates of the constructed model using mean height derived from the LIDAR DSM at various grid resolutions can be examined. Section 4.2 contains a discussion of the result of this analysis.

Case III

For Case III, the 3D model was constructed using the maximum height derived from the LIDAR DSM at various grid resolutions. A 3D model constructed using the maximum height from the 2m-grid resolution LIDAR DSM was adopted as control. The hypothesis posed is that, for roof with one dominant height the *RMSE* computed will be constant, even though the model is constructed with varying grid resolutions. The computed discrepancies in this case are of the same order. Therefore, the role of grid resolution in preserving the accuracy estimates of the constructed model using maximum height derived from the LIDAR DSM at various grid resolutions can also be examined (section 4.3).

The procedure for the computation of *RMSE* is shown in Figure 10. Due to the potential locational mismatch between the building polygons and the LIDAR DSM, the derived heights (mean height from LIDAR DSM) used to construct the 3D model could be in error. Figure 11 shows an example of the mismatch between the building polygons and the corresponding buildings on the LIDAR DSM. Due to the mismatch, errors in the retreived heights at building edges on the LIDAR DSM could affect the computation of the derived height, where the height of the ground surface could be incorperated in the computation (Figure 11).

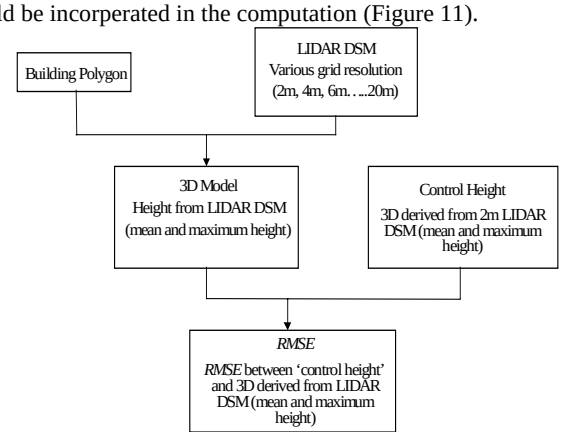

Figure 10: The procedure for the computation of *RMSE*.

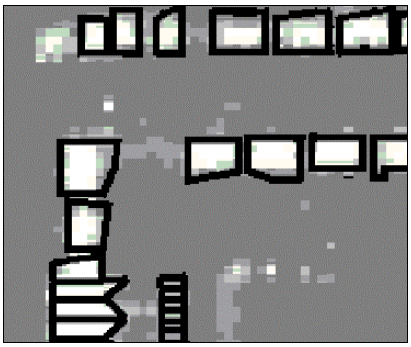

Figure 11: Mismatch between the building polygons and the LIDAR DSM.

3.2 Standard Deviation (*Std. Dev*.)

For the computation of *Std. Dev*., the formula used is as shown in Equation 2. The "Zonalstat" function available within ARC/INFO is used to compute the *Std. Dev*. using the building polygon as a 'mask'. As stated above, the potential locational mismatch between the building polygon and the LIDAR DSM could also affect the computation of the *Std. Dev*. because the heights of ground surface locations may erroneously be placed within the building polygon (Figure 10).

$$Std.\ Dev.\ (\sigma) = \sqrt{\frac{\sum \left(z - \bar{z}\right)^2}{n}} \qquad [2]$$

where n is the number of grid within a building polygon , $\bar{z}$ is the mean height for the building polygon and z is the height value for each grid within the building polygon.

Further discussion of the variation of *Std. Dev*. on the building heights at various LIDAR DSM grid resolutions can be found in section 4.5.

4 RESULTS AND DISCUSSION

4.1 Maximum height derived from LIDAR DSM and mean height as control

It was noted in 3.1 (Case I) that the *RMSE* is not related to the 'absolute' accuracy estimates but rather is used to detect relative height changes. Figure 12 shows the vertical roof heights for residential and industrial buildings for the derived 3D model at different grid resolutions.

The vertical roof height for both residential and industrial buildings decreases gradually as the grid resolution of the LIDAR DSM increases (Figure 12). However, there is a difference between the vertical roof heights of residential and industrial buildings, the vertical roof height of residential buildings decreases from 2.4m to 1.3m as the LIDAR DSM grid resolution increases from 2m to 20m (Figure 12). On the other hand, even

though the vertical roof height of industrial buildings decreases as the grid resolution increases, it consistently shows a higher vertical roof height compared to residential buildings. The values for the computed vertical roof height are between 4.1m and 2.4m as the grid resolution increases. It appears, therefore, from Figure 12, that industrial buildings have a higher vertical roof height compared to residential buildings. Differentiation of the two building types by analysing the vertical roof height at various grid resolutions between 2m to 20m seems possible. It is also found that, the maximum difference between the computed vertical roof height (1.70m) is experienced at 2m-grid resolution. It is suggested that differentiating the building type at a smaller grid resolution (less than 2m) will improve the result. This is due to the fact that more height values will be available from the LIDAR DSM and the possibilities of detecting the 'true' maximum height of both building types is therefore greater. Further studies in relation to this effect will be carried out. In general, it is shown that the vertical roof height that corresponds to industrial buildings is higher than residential buildings.

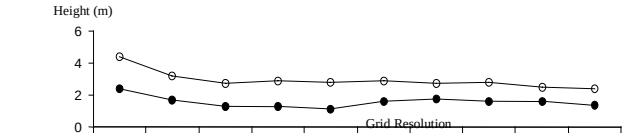

	2m	4m	6m	8m	10m	12m	14m	16m	18m	20m
Residential	2.4	1.7	1.3	1.3	1.2	1.6	1.8	1.6	1.6	1.3
Industrial	4.1	3.2	2.7	2.9	2.8	2.9	2.7	2.8	2.5	2.4

Figure 12: Vertical roof heights for the residential and industrial buildings (Maximum height derived from the LIDAR DSM to construct the 3D model and for control height, 3D model constructed using the mean height from 2m-grid resolution LIDAR DSM).

4.2 Mean height derived from LIDAR DSM and mean height as control

As noted in Section 3.1 (Case II), apart from using the maximum height from the LIDAR DSM to construct the 3D model, the use of mean height is also analysed. In this case, apart from understanding the roof height differences between the two building types, accuracy estimates for the derived model using the mean height from the LIDAR DSM are known. It is shown that grid resolution in the LIDAR DSM plays an important role in constructing the 3D model. The accuracy estimates for both building types constructed using the mean height from the LIDAR DSM increases as the grid resolution increases (Figure 13).

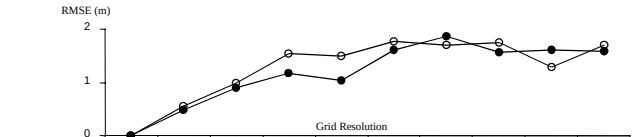

	2m	4m	6m	8m	10m	12m	14m	16m	18m	20m
Residential	0	0.5	0.9	1.2	1.0	1.6	1.9	1.6	1.6	1.6
Industrial	0	0.5	1.0	1.5	1.5	1.8	1.7	1.7	1.3	1.7

Figure 13: *RMSE* for the residential and industrial building (mean height derived from the LIDAR DSM to construct the 3D model and for control height, 3D model constructed using the mean height from 2m-grid resolution LIDAR DSM).

Figure 13 shows that both building types exhibit an increase in *RMSE* as the 3D model is constructed with an increase in LIDAR DSM grid resolution. This indicates that the roof structure of both of the building types is not flat and shows some variation in height. The industrial buildings, in general, have a slightly higher *RMSE* compared to residential buildings.

4.3 Maximum height derived from LIDAR DSM and maximum height as control

Figure 14 shows the *RMSE* plot for the residential and industrial buildings when the maximum height is used to construct the 3D models at various grid resolutions. The control height adopted in Case III is the height of a 3D model constructed using the maximum height from the 2m-grid LIDAR DSM.

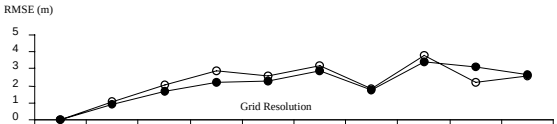

	2m	4m	6m	8m	10m	12m	14m	16m	18m	20m
Residential	0	0.9	1.7	2.2	2.2	2.9	1.7	3.4	3.1	2.7
Industrial	0	1.1	2.0	2.9	2.6	3.2	1.8	3.8	2.2	2.5

Figure 14: *RMSE* for the residential and industrial building (maximum height derived from the LIDAR DSM to construct the 3D model and for control height, 3D model constructed using the maximum height from 2m-grid resolution LIDAR DSM).

Figure 14 shows that the *RMSE* for residential and industrial buildings increases as the grid resolution increases. In these plots, there are no distinct differences between the pattern of *RMSE* for residential and industrial buildings. However, industrial buildings appear to exhibit higher *RMSE* values compared to residential buildings. One of the advantages observed from Figures 13 and 14 is that *RMSE* values computed using the mean height derived from the LIDAR DSM (Figure 13) are much smaller compared to the equivalent values derived using the maximum height (Figure 14). It appears that 3D models constructed using the mean height from the LIDAR DSM are more reliable than using the maximum height. This is due to the fact that the mean height reduces the risk that derived building heights are influenced by localised high points such as tall chimneys or by the inclusion of adjacent ground heights resulting from mismatch between the LIDAR data and the polygon data. However, for certain applications, such as the computation of inter-visibility between two points or telecommunications applications, the use of maximum height from the LIDAR DSM to construct the 3D model would be more appropriate.

4.4 Maximum height derived from LIDAR DSM and mean height as control for individual buildings

Referring to Figures 12 to 14, it can be concluded that there is some sort of typical variation in vertical roof height for both building type. Industrial buildings appear to have a higher

vertical roof height than residential buildings. Categorising the building types using *RMSE* as discussed in section 4.1 to 4.3 therefore appears to be possible. Even though there is difference in roof height between the two building types, could the complexity of the roof structure be examined to a certain extent?

To investigate this idea further, the height difference between the derived height from the 3D models constructed at various grid resolutions, and a control height is determined. In this case, the 3D model is constructed using the maximum height derived from the LIDAR DSM from 2m to 10m in grid resolution. For the control height, a 3D model constructed using the 2m-grid resolution LIDAR DSM was used. Four randomly selected residential and industrial buildings are identified. Figure 15 and Figure 16 shows the difference between the derived height and the control height for the selected building using a grid resolution of between 2m and 10m with 2m-grid interval for the residential and industrial buildings respectively. There is a distinct difference between the two plots corresponding to the residential and the industrial buildings. From Figure 15, it is clear that the residential buildings (a, b, c, and d) exhibit a high variation in height (derived height – control height) as LIDAR DSM grid resolution increases. This is due to the complex roof structure of residential buildings, which have roofs of varying shape and height. For industrial buildings (j, k, l, and m), the variation seems to be more consistent beyond a grid resolution of 4m, as shown in Figure 16. This effect might be due to the fact that the roof structures of industrial buildings are less complex (i.e., exhibit less height variation). Categorising building type by analysing the difference between the derived height and the control height for each building as illustrated in Figure 15 and Figure 16 seems possible.

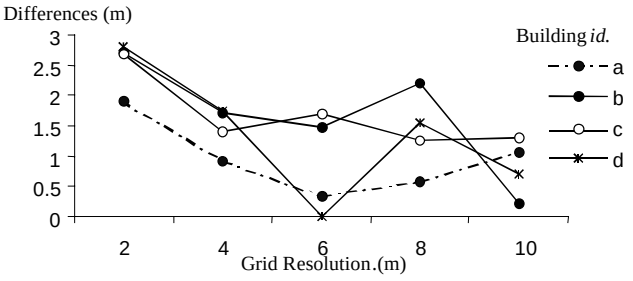

Figure 15: The difference between derived height and control height for residential buildings.

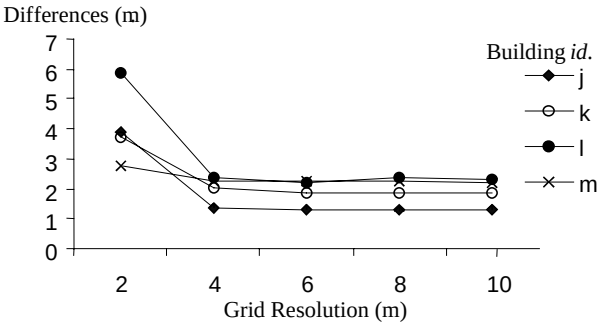

Figure 16: The difference between derived maximum height and control height for industrial buildings.

4.5 Effect of Standard Deviation (*Std. Dev.*) on building height

In the final part of the study, the variation of the *Std. Dev*. measure for residential and the industrial buildings at various LIDAR DSM grid resolutions is investigated. Figure 17 shows the computed *mean Std. Dev*. for two samples of size 35 and 7 for residential and industrial buildings respectively at various grid resolutions. There is a distinct difference between the computed *mean Std. Dev.* for residential and industrial buildings. The computed *mean Std. Dev*. for residential building decreases sharply from 1.6m to zero as grid resolution increases from 2m to 14m. This is partly because the surface area of residential buildings is small, and so the value of the *mean Std. Dev*. converges to zero as a result of averaging as the grid resolution increases. However, for industrial buildings, the computed *mean Std. Dev*. decreases steadily from 2m to 1.1m as grid resolution increases from 2m to 16m and is almost constant beyond a 16m-grid resolution. This is probably due to the large surface area of industrial buildings, which gives a more consistent *mean Std. Dev*. over this range of cell resolutions. Therefore, if the size of the building is a significant factor in categorisation, understanding the effect of *mean Std. Dev*. at various grid resolutions appears to be a reasonable approach.

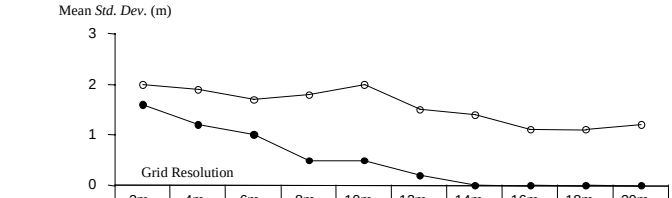

	2m	4m	6m	8m	10m	12m	14m	16m	18m	20m
Residential	1.6	1.2	1	0.5	0.5	0.2	0	0	0	0
Industrial	2	1.9	1.7	1.8	2	1.5	1.4	1.1	1.1	1.2

Figure 17: Mean *Std. Dev*. for residential and industrial building at various grid resolutions.

Furthermore, since there is a distinct difference between the *mean Std. Dev.* for residential and industrial buildings at various grid resolutions, the ability of the *Std. Dev*. measure to identify individual buildings is also investigated for randomly selected buildings from each site.

Figure 18 shows the computed *Std. Dev.* for residential buildings using grid resolutions ranging from 2m to 10m. The *Std. Dev*. for each residential building (p, q, r and s) converges to zero at a grid resolution of 10m. As mentioned earlier, this is due to the effects of averaging. On the other hand, due to the complexity of the roof shape of the residential buildings, significant variation in *Std. Dev.* is seen at grid resolutions between 2m and 10m. Figure 19 depicts the computed *Std. Dev*. for the selected industrial building (t, u, v and w) using grid resolutions of 2m to 10m. The computed *Std. Dev*. values are almost constant in the industrial buildings between grid resolutions of 2m to 10m. This is partly due to the low-complexity of the roof structures as well as the greater surface areas of industrial buildings. The behaviour of the *Std. Dev*. for individual buildings appears to reveal properties of the

nature of the roof type and thus assist in discriminating between the two building types.

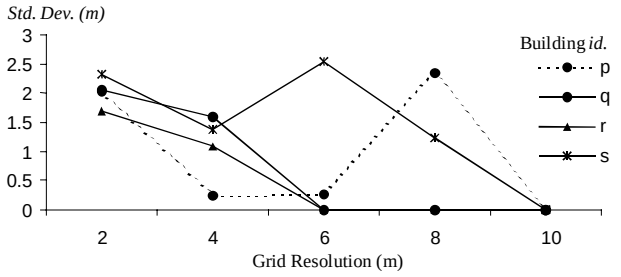

Figure 18: *Std. Dev*. for selected residential buildings (p, q, r and s) using 2m to 10m grid resolution LIDAR DSM.

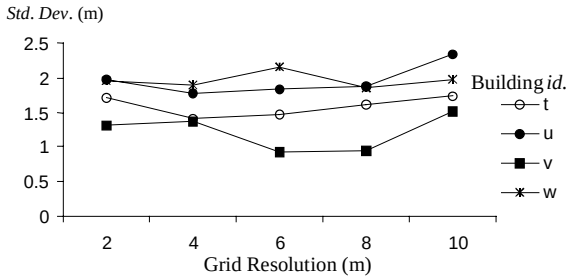

Figure 19*: Std. Dev.* for selected industrial building (t, u, v and w) at 2m to 10m grid resolution LIDAR DSM.

5 CONCLUSIONS

Differentiating between residential and industrial building types using simple statistics such as *RMSE* and *Std. Dev*. is shown to be possible. The findings of this study may provide a basis for categorising residential and industrial building types in a more automated fashion. The main findings of this study are:

- By examining the effect of *RMSE* on 3D models at various LIDAR DSM grid resolutions, the differences between roof structures of residential and industrial buildings can be inferred.

- The complexity of the roof structures of the two building types can be examined using the *Std. Dev*. measure on individual buildings at various LIDAR DSM grid resolutions.

- The use of mean height from LIDAR DSM to construct 3D models using the integrated methodology results in smaller *RMSE* compared to the use of the maximum height.

- Categorising the two building types using *RMSE* at various grid resolutions reveals the vertical roof heights and might be useful for certain applications.

ACKNOWLEDGEMENTS

The authors wish to thank the National Centre for Environmental Data and Surveillance, Environment Agency, Bath, England, who provided the LIDAR datasets. The Ordnance Survey of Great Britain kindly provided Land Line dataset. University Technology MARA, Malaysia, is supporting Mr. Jaafar's research project. Research and computing facilities were made available by the School of Geography, The University of Nottingham.

REFERENCES

Gruen, A., Kubler, O., and Agouris, P., (eds), 1995. Automatic extraction of man-made objects from aerial and space images, Birkhauser Verlag, Basel.

Gruen, A., Baltsavias, E. P., and Henricsson, O., (eds), 1997. Automatic extraction of man-made objects from aerial and space images (II), Birkhauser Verlag, Basel.

Haala, N. and Brenner, C., 1999. Generation of virtual city models using laser altimetry, 2D GIS, unwrapping of detailed surface model. GIM International, Vol. 13, No. 3, pp. 6-8.

Hug, C., 1996. Combined use of laser scanner geometry and reflectance data to identify surface objects. OEEPE-Workshop '3D city models', Bonn, Germany, 9 – 11 October 1996.

Jaafar, J., Priestnall, G., Mather, P.M. and Vieira, C.A., 1999a. Construction of DEM from LIDAR DSM using morphological filtering, conventional statistical approaches and Artificial Neural Networks. RSS'99 - Earth Observation, From data to information, Proceedings of the 25th Annual Conference and Exhibition of the Remote Sensing Society, Cardiff, 8-10 September 1999, pp. 299-306. Remote Sensing Society, Nottingham.

Jaafar, J., Priestnall, G. and Mather, P.M., 1999b. Assessing the effects of grid resolution in laserscaning datasets towards the creation of DSMs, DEMs and 3D models. Presented at the Fourth International Airborne Remote Sensing Conference and Exhibition/21st Canadian Symposium on Remote Sensing, Ottawa, Ontario, Canada, 21-24 June 1999, pp. 606-613.

Lohr, U., 1998. Laserscanning for DEM generation, In: GIS technologies and their environmental applications, Brebbia C. A. and Pascolo P. (eds). Computational Mechanics Publications, Southampton, pp. 243-249.

Wehr, A. and Lohr, U., 1999. Airborne laser scanning – an introduction and overview. ISPRS Journal of Photogrammetry and Remote Sensing, 54, pp. 68-82.